Microelectronic Engineering 98 (2012) 453–457

Contents lists available at SciVerse ScienceDirect

Microelectronic Engineering

journal homepage: www.elsevier.com/locate/mee

Development and characterization of a needle-type microelectrode array for stimulation and recording of neuronal activity

S. Röhler [a,*], J. Held [a], W. Nisch [a], D.P. Kern [b], C. Burkhardt [a], A. Stett [a]

[a] NMI Natural and Medical Sciences Institute, Markwiesenstraße 55, 72770 Reutlingen, Germany
[b] Institute of Applied Physics, University of Tuebingen, Auf der Morgenstelle 10, 72076 Tuebingen, Germany

ARTICLE INFO

Article history:
Available online 24 July 2012

Keywords:
Microelectrode array
Needle-type electrodes
Neurochip
Neuronal activity
SU-8
Dry etching

ABSTRACT

Arrays of needle-type electrodes are expected to surpass arrays of planar electrodes used for measuring neuronal activity or stimulation of neurons concerning properties like stimulation threshold, spatial resolution and signal-to-noise ratio. This work describes the fabrication of such needle-type electrodes. The three-dimensionally shaped electrodes are 50 μm high. Typical values for the base diameter are 20 μm and a few microns for the tip radius. The needles are fabricated from cross-linked SU-8 using dry etching. Gold and titanium are used as metallization and SiO_xC_y as insulator. The tips of the electrodes are covered with nano-columnar titanium nitride.

1. Introduction

1.1. Microelectrode arrays

Microelectrode arrays (MEAs) with substrate-integrated planar microelectrodes have been used since the early 70 s [1] to stimulate and measure the activity of neurons in cell and tissue culture experiments. It is possible to investigate the properties of neuronal networks with MEAs [2,3]. Also implantable devices like retina implants make use of a MEA to stimulate neuronal tissue [4]. With MEAs extracellular potentials are recorded at the two-dimensional interface between the electrodes and the tissue. Typically, cellular signal sources are located within a radius of about 30 μm around the electrode center.

For the fabrication of these devices only biocompatible materials may be used. This means that the behavior of the cells that are in contact with the MEA may not be influenced by the materials. Furthermore the materials must be biostable: they may not dissolve or corrode when they are in contact with tissue or electrolytes. MEAs should survive a sterilization procedure before usage [5]. Fig. 1 schematically shows the functional principle of a MEA.

In case of recording from acute brain slices which exhibit a layer of dead cells at the surface the signal-to-noise ratio is decreased and only from a few cells action potentials can be recorded. Applications with electrical stimulation suffer from a similar problem: Mostly the cells targeted for excitation are located inside the tissue volume around the electrode at a certain distance from the planar electrode surface and the stimulation strength has to be increased at the expense of spatial resolution and energy consumption of implants.

1.2. Needle-type electrodes

To counteract these issues we developed a MEA with needle-type microelectrodes. These protruding electrodes are able to penetrate tissue. This shortens the distance between the electrically active cells and the active electrode area for recording or between the stimulating electrode and the stimulated cell, respectively. Our method allows the use of different types of substrates because the needles are fabricated on top of the substrate. This is advantageous compared to fabrication processes described by others that are restricted to a certain substrate type like glass [6] or silicon [7–9]. As mentioned above for the whole device only biocompatible materials may be used.

2. Fabrication process

Fig. 2 gives an overview of the fabrication process. The substrate is covered with cross-linked SU-8 and a metal layer (Fig. 2a). This metal layer is patterned so that it serves as an etch mask (Fig. 2b). The SU-8 is etched so that cones remain on the substrate (Fig. 2c). With a second lithography step another metal layer is deposited from which the electrical connection between the contact pads on the substrate and the needle tips are made (Fig. 2d). Then the needles and the conductors are insulated (Fig. 2e) and embedded into photoresist, followed by a third,

* Corresponding author.
E-mail addresses: sebastian.roehler@nmi.de, sebastian.roehler@googlemail.com (S. Röhler).

0167-9317/$ - see front matter © 2012 Elsevier B.V. All rights reserved.
http://dx.doi.org/10.1016/j.mee.2012.07.104

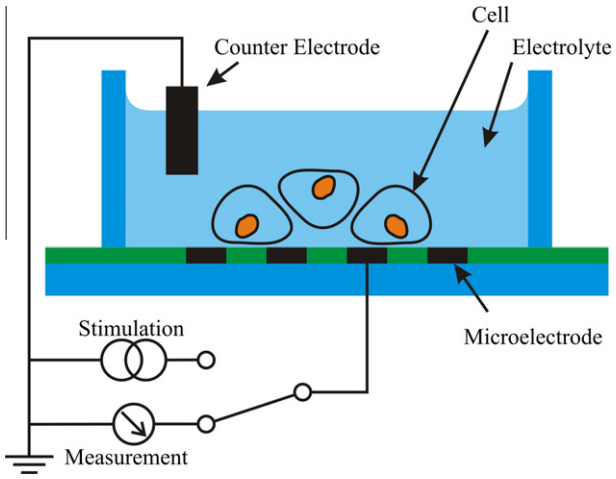

Fig. 1. Schematic drawing of a MEA with planar electrodes used for stimulation or measurement of neuronal activity.

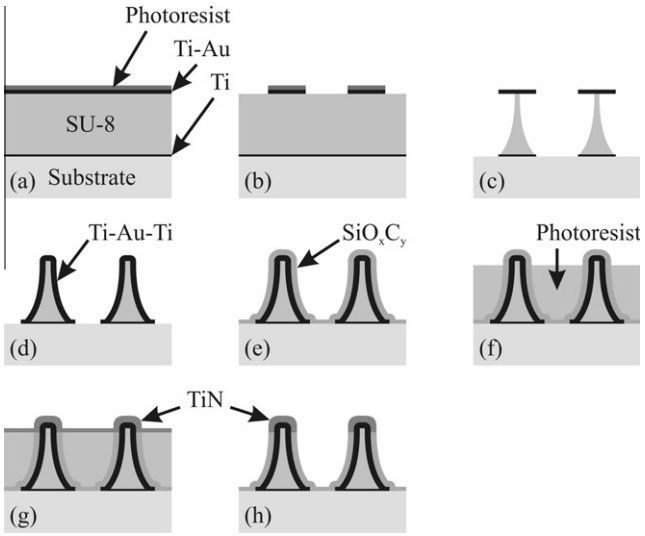

Fig. 2. Schematic overview of the fabrication process: (a) substrate preparation, (b) etching mask definition, (c) needle etching, (d) metallization, (e) insulation, (f) embedding in photoresist, (g) needle opening and deposition of electrode material and (h) lift-off.

maskless lithography step to open up the needle tips (Fig. 2f) in order to remove the insulator at the tips. Finally the needle tips are covered with the electrode material in a lift-off process (Fig. 2g and h).

2.1. Substrate preparation

For the fabrication of MEAs with three-dimensionally shaped electrodes different substrates can be used like silicon, glass or flexible substrates. For the process described in this work we used silicon wafers and float glass slides. The substrate is cleaned and a 20 nm thick titanium (Ti) layer is sputtered for better adhesion of SU-8 onto the substrate. Then a 50 μm thick layer of the negative photoresist SU-8 is spun onto the substrates. To cross-link the SU-8 a flood exposure and a hard bake at 150 °C are performed. The resist is covered with a 20 nm thick titanium layer and a 400 nm thick gold (Au) layer. This metal layer is patterned using physical dry etching in an argon plasma. The metal is used as a hard mask for etching the SU-8.

2.2. SU-8 etching

The etching process is performed in the plasma etching system Z401 (Leybold). A mixture of oxygen (O_2) and tetrafluoromethane (CF_4) is used as etching gas. The radio frequency generator for the plasma is operated at 13.56 MHz. To determine the influence of pressure, bias voltage, O_2/CF_4 ratio and total gas flow on horizontal and vertical etch rates, in different etching series each one of these parameters was varied while keeping the others constant at the following values: pressure: 10 Pa, bias voltage: 300 V, O_2/CF_4 ratio: 10:1, gas flow: 55 sccm. If r_h is the horizontal etch rate and r_v the vertical etch rate then the anisotropy A is defined as

$$A = \frac{r_v - r_h}{r_v}.$$

The hard mask used to etch the SU-8 consists of solid disks with a diameter of 40 μm. After the etching step the tip radius of the needles should be only a few microns. This means that in the etching process the anisotropy must be slightly greater than 0.6. Fig. 3 shows the result of the etching series. The pressure has a strong influence on the etch rates: the higher the pressure, the higher the etch rates (Fig. 3a) and the lower the roughness. If the bias voltage is increased, the vertical etch rate rises but the horizontal etch rate remains constant (Fig. 3b). This means that the anisotropy can be raised by increasing the bias voltage. But a higher bias voltage leads also to increased roughness and etch mask erosion. By enlarging the amount of CF_4 in the etch gas, the anisotropy can be enhanced (Fig. 3c). The total flow of the etch gases hardly has an influence on etch rate and anisotropy (Fig. 3d) but higher flow achieves smoother sidewalls of the needles.

Based on these results the following process is chosen to etch the needles from a 50 μm thick SU-8 layer: pressure: 10 Pa; bias voltage: 430 V; gases: 100 sccm O_2, 20 sccm CF_4; etching time: 115 min. To reduce heating of the substrates the substrate plate is water cooled. Subsequent to this step the etching residues and the remaining etch masks are removed in isopropyl alcohol with the aid of ultrasound. Fig. 4 shows a scanning electron microscope (SEM) image of an array of etched needles. There is a good uniformity of the shape of the needles in the array and between the needles there are no SU-8 residues on the substrate.

2.3. Metallization and insulation

The needles are metalized with a sputtered layer stack of Ti (20 nm), Au (400 nm) and again Ti (20 nm). This metallization is used to cover the sidewalls of the needle and to form conductor paths so that an electrical connection between contact pads on the substrate and the needle tips is created. The first Ti layer serves as an adhesion promoter between the substrate or the SU-8 and the Au layer and the upper Ti layer as an adhesion promoter between the Au layer and the later deposited insulation. The metallization is structured using a thick photoresist that is spun with a thickness of 60 μm onto the substrate. This high thickness is necessary because the needles have to be covered completely by the photoresist. The upper Ti layer is etched in Ar/CF_4 plasma, the Au layer in Ar plasma and the lower Ti layer again in Ar/CF_4 plasma. Afterwards the resist is removed.

A SiO_xC_y layer is deposited as insulator in a plasma-enhanced chemical vapor deposition (PECVD) process from a hexamethyldisiloxane (HMDSO) precursor. This step was performed in a CVD-Piccolo (Plasma Electronic). It turned out that this SiO_xC_y layer provides better adhesion and less leakage current than reactively sputtered silicon nitride (SiN). A maskless lithography step is used to remove the insulator at the tips of the needles. For this purpose the needles are again embedded into a thick positive tone photoresist. After a short flood exposure the resist is removed in the devel-

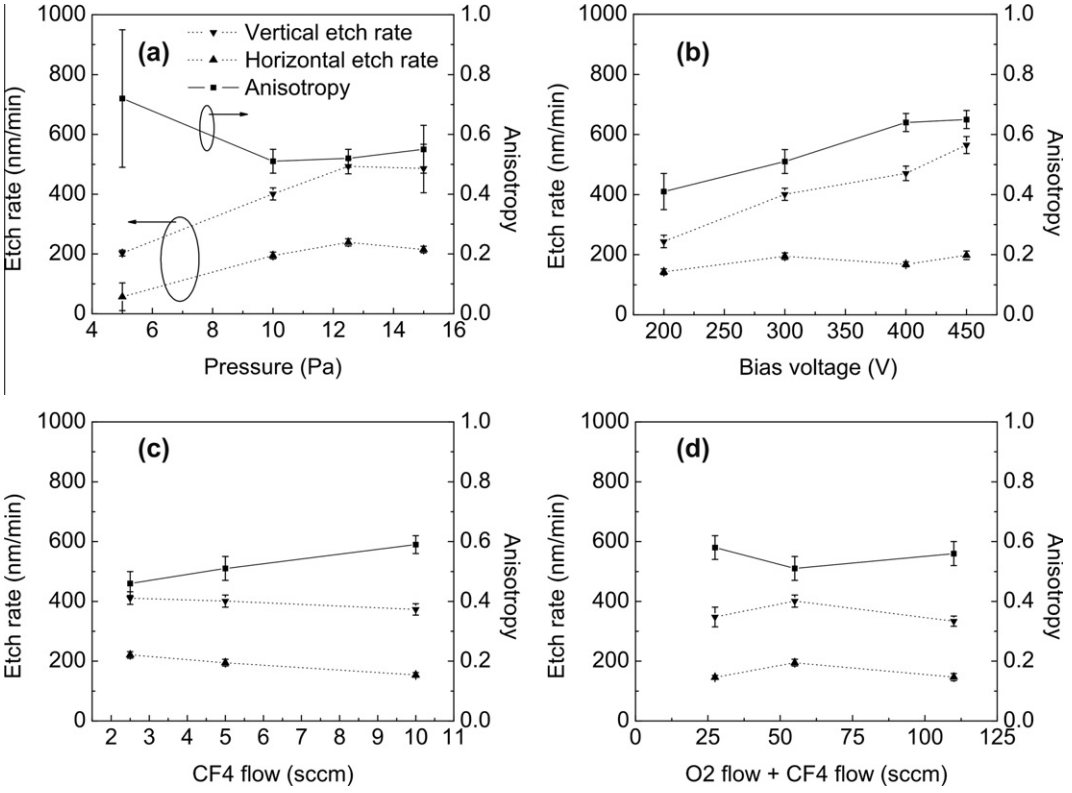

Fig. 3. Dependence of the vertical etch rate, horizontal etch rate and the anisotropy on (a) pressure, (b) bias voltage, (c) O_2/CF_4 ratio and (d) gas flow.

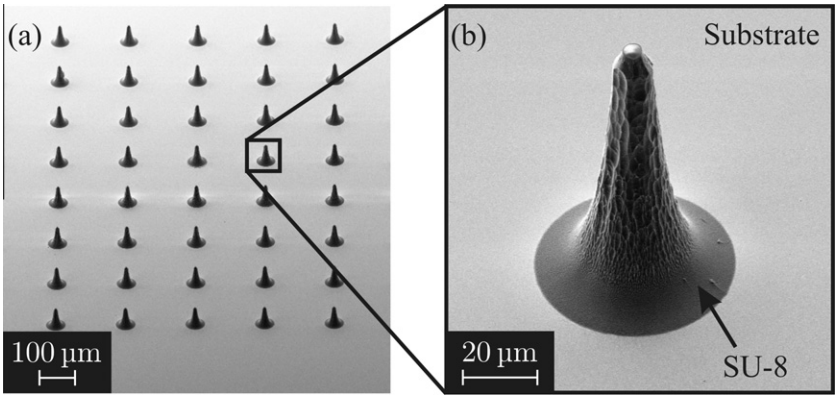

Fig. 4. SEM image of (a) an array of etched needles and (b) close up of a single needle.

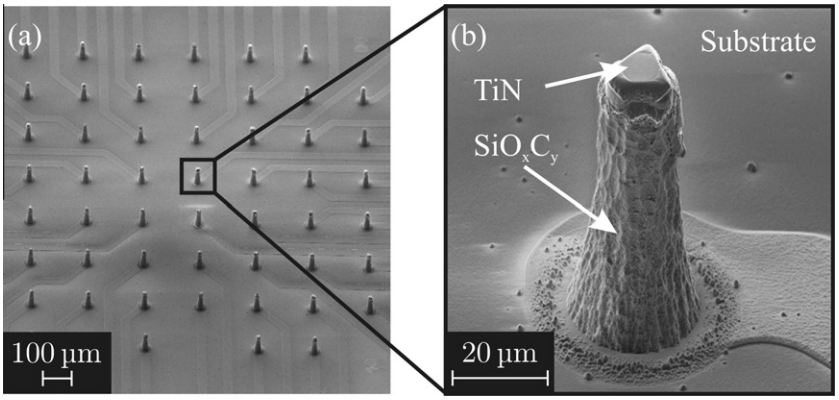

Fig. 5. SEM image of (a) an array of needle-type microelectrodes after TiN lift-off and (b) close up of a single needle.

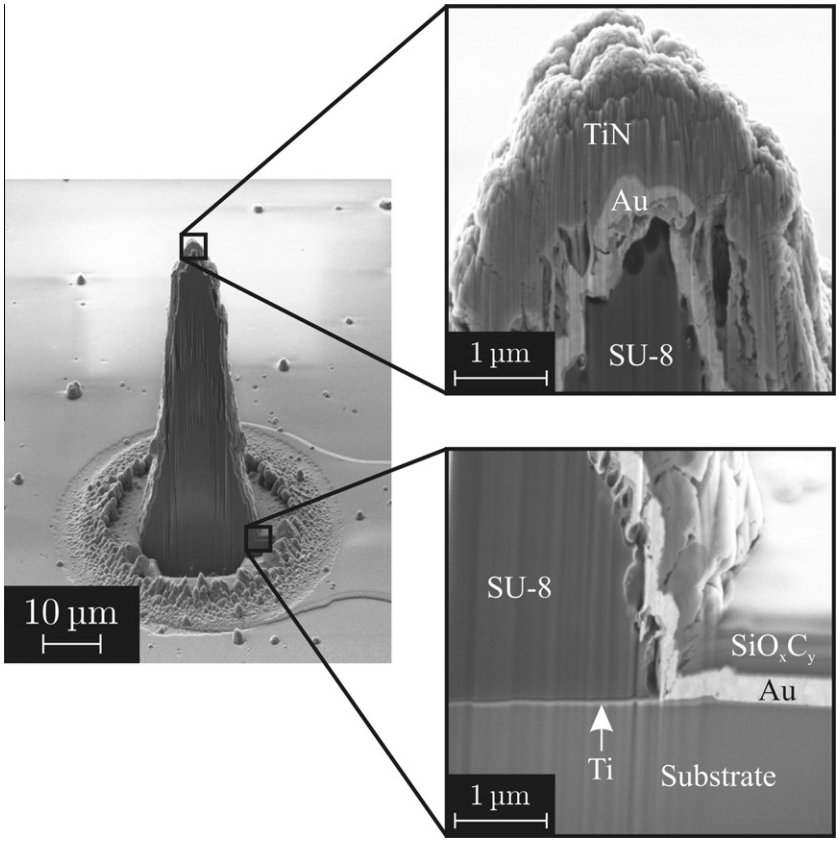

Fig. 6. SEM images of a needle-type microelectrode after FIB preparation.

oper only at the needle tips. With a subsequent etch back in O_2 plasma resist residues at the tips are removed. The duration of flood exposure and etch back determines how much of the sidewalls are still covered with resist. To prepare the deposition of the electrode material at the tip of the needle the SiO_xC_y is etched in O_2/CF_4 plasma with the underlying Au layer as an etch stop.

2.4. Electrodes

After opening the needle tips the resist is not removed but it is used for a lift-off process. Nano-columnar titanium nitride (TiN, 600 nm) is sputtered on the samples. This ensures low impedances because of the high electrochemical surface area of TiN [10,11]. When the resist is removed in acetone the TiN remains only at the needle tips. In O_2 plasma the electrodes are rendered hydrophilic. Fig. 5 shows a SEM image of the finished array after TiN lift-off. The Ti-Au-Ti conductor paths visible in this image are covered with the SiO_xC_y insulator.

3. Characterization

The active geometric surface area of the electrode shown in Fig. 5 was approximately 580 µm^2. The microneedles were investigated in the combined focused ion beam (FIB) and SEM Auriga® (Carl Zeiss Microscopy). FIB preparation was used to uncover the layer structure at the needle tip and sidewall shown in the SEM image in Fig. 6. This image shows that there is a good electrical contact between the electrode at the tip and the Ti–Au–Ti conductor paths on the substrate. At the sidewalls the Ti–Au–Ti layer is well covered by the insulator. At the tip the TiN shows the desired nano-columnar structure.

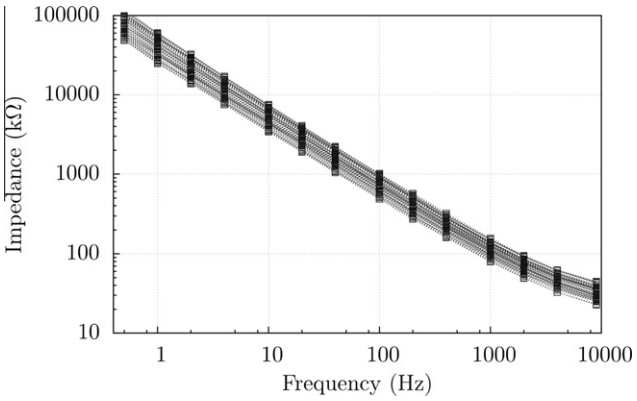

Fig. 7. Overlaid impedance spectra of an array of 59 needle-type microelectrodes.

Fig. 7 shows overlaid impedance spectra of an array of 59 electrodes with this geometry. The mean impedance at 1 kHz is 115 kΩ with a standard deviation of 25 kΩ. This impedance is slightly higher than that of a planar TiN electrode with a diameter of 30 µm which exhibits an impedance of 30–40 kΩ but should be acceptable for neuronal activity measurements.

4. Conclusion

In summary, we developed a process to fabricate arrays with needle-type microelectrodes on different substrates for recording and stimulating nerve cell activity inside of neuronal tissue. The height of the needles is determined by the thickness of the SU-8 layer from which the needles are fabricated and typically amounts

to 50 μm. Typical values for the base diameter are 20 μm and a few microns for the tip radius. The part of the surface of the microneedle used as an electrode is defined by a maskless lithography step. Nano-columnar titanium nitride is used as electrode material.

Acknowledgment

This work was supported by the Federal Ministry of Education and Research (BMBF), Grant 0312035A.

References

[1] C.A. Thomas, P.A. Springer, G.E. Loeb, Y. Berwald-Netter, L.M. Okun, Exp. Cell Res. 74 (1972) 61–66.
[2] A. Stett, U. Egert, E. Guenther, F. Hofmann, T. Meyer, W. Nisch, H. Haemmerle, Anal. Bioanal. Chem. 377 (2003) 486–495.
[3] M. Fejtl, A. Stett, W. Nisch, K.-H. Boven, A. Möller, On micro-electrode array revival: its development, sophistication of recording, and stimulation, in: M. Taketani, M. Baudry (Eds.), Advances in Network Electrophysiology, Springer, New York, 2006, pp. 24–37.
[4] E. Zrenner, K.U. Bartz-Schmidt, H. Benav, D. Besch, A. Bruckmann, V.-P. Gabel, F. Gekeler, U. Greppmaier, A. Harscher, S. Kibbel, J. Koch, A. Kusnyerik, T. Peters, K. Stingl, H. Sachs, A. Stett, P. Szurman, B. Wilhelm, R. Wilke, Proc. R. Soc. B 278 (2011) 1489–1497.
[5] H. Hämmerle, U. Egert, A. Mohr, W. Nisch, Biosens. Bioelectron. 9 (1994) 691–696.
[6] M.O. Heuschkel, M. Fejtl, M. Raggenbass, D. Bertrand, P. Renaud, J. Neurosci. Meth. 114 (2002) 135–148.
[7] P. Thiébaud, C. Beuret, N.F. de Rooij, M. Koudelka-Hep, Sens. Actuators B 70 (2000) 51–56.
[8] J. Held, J. Gaspar, P. Ruther, M. Hagner, A. Cismak, A. Heilmann, O. Paul, J. Micromech. Microeng. 20 (2010) 025024.
[9] G. Charvet, L. Rousseau, O. Billoint, S. Gharbi, J.-P. Rostaing, S. Joucla, M. Trevisiol, A. Bourgerette, P. Chauvet, C. Moulin, F. Goy, B. Mercier, M. Colin, S. Spirkovitch, H. Fanet, P. Meyrand, R. Guillemaud, B. Yvert, Biosens. Bioelectron. 25 (2010) 1889–1896.
[10] M. Janders, U. Egert, M. Stelzle, W. Nisch, in: Engineering in Medicine and Biology Society (EMBC), Annual Int. Conf. of the IEEE, Amsterdam, Netherlands, 1996, pp. 245–247.
[11] S.F. Cogan, Ann. Rev. Biomed. Eng. 10 (2008) 275–309.